International Journal of Remote Sensing
Vol. 26, No. 19, 10 October 2005, 4381–4398

Taylor & Francis
Taylor & Francis Group

Time-series validation of MODIS land biophysical products in a Kalahari woodland, Africa

K. F. HUEMMRICH*†, J. L. PRIVETTE‡, M. MUKELABAI§, R. B. MYNENI¶ and Y. KNYAZIKHIN¶

†Joint Center for Earth Systems Technology, University of Maryland, Baltimore County, Baltimore, MD 20771, USA

‡Code 614.4, Biospheric Sciences Branch, NASA Goddard Space Flight Center, Greenbelt, MD 20771, USA

§Meteorological Office, Mongu, Zambia

¶Department of Geography, Boston University, MA 02215, USA

Monthly measurements of leaf area index (LAI) and the fraction of absorbed photosynthetically active radiation (f_{APAR}) taken at approximately monthly intervals were collected along three 750 m transects in a Kalahari woodland near Mongu in western Zambia. These data were compared with MODIS NDVI (MOD13, Collection 3) and MODIS LAI and f_{APAR} products (MOD15, Collection 3) over a 2 year period (2000–2002). MODIS and ground-measured LAI values corresponded well, while there was a significant bias between MODIS and ground-measured f_{APAR} even though both MODIS variables are produced from the same algorithm. Solar zenith angle effects, differences between intercepted and absorbed photosynthetically active radiation, and differences in measurement of f_{APAR} (photon counts versus energy) were examined and rejected as explanations for the discrepancies between MODIS and ground-measured f_{APAR}. Canopy reflectance model simulations produced different values of f_{APAR} with the same LAI when canopy cover was varied, indicating that errors in the estimation of canopy cover in the MODIS algorithm due to the land cover classification used are a possible cause of the f_{APAR} discrepancy. This is one of the first studies of MODIS land product performance in a time-series context. Despite a bias in f_{APAR}, our results demonstrate that the woodland canopy phonology is captured in the MODIS product.

1. Introduction

One of the important uses of satellite observations of the Earth is to monitor seasonal changes of vegetation (e.g. Goward *et al.* 1985, Justice *et al.* 1985, Reed *et al.* 1994, Moulin *et al.* 1997, Chidumayo 2001). Seasonal variations in leaf area index (LAI) and the fraction of absorbed photosynthetically active radiation (f_{APAR}) are vital to determine landscape water, energy and carbon balances, as well as in the detection of long-term climate change (Potter *et al.* 1993, Churkina and Running 1998). As such, it is useful to examine the accuracy of LAI and f_{APAR} from the MODIS (Moderate-Resolution Imaging Spectroradiometer) algorithms against surface measurements over a multi-year period at a single site that experiences significant seasonal variations in these variables.

*Corresponding author. Email: karl.huemmrich@gsfc.nasa.gov

International Journal of Remote Sensing
ISSN 0143-1161 print/ISSN 1366-5901 online
http://www.tandf.co.uk/journals
DOI: 10.1080/01431160500113393

In any exercise where there are comparisons made between biophysical variables measured using multiple methods, it is very important to understand how each variable is defined as well as to examine the effects of possible error sources affecting the measurements.

There are multiple approaches to measuring LAI, and along with them are multiple subtly different definitions of LAI itself. Barclay (1998) describes five common measurement approaches for determining LAI and finds that each measurement approach results in a different definition of LAI. His five definitions are:

1. total LAI based on the total outside area of the leaves, taking leaf shape into account, per unit area of horizontal land below the canopy;
2. one-sided LAI is generally defined as half the total LAI, even where the two sides of the leaves are not symmetrical;
3. horizontally projected LAI is the area of 'shadow' that would be cast by each leaf in the canopy with a light source at infinite distance and perpendicular to it, summed up for all leaves in the canopy per unit area of horizontal land below the canopy;
4. inclined projected LAI, 'silhouette' LAI, or effective LAI, represents the projected area of leaves taking into account individual leaf inclinations; and
5. a variation on number 4 where overlapping leaf areas are counted only once.

With each of these definitions of LAI, there are associated ground-based measurement approaches (Scurlock *et al.* 2001):

a. destructive harvesting and direct determination of one-sided leaf area, using squared grid paper, weighing of paper replicates, or an optically based area measurement system;
b. collection and weighing of total leaf litterfall, converted to leaf area by determining specific leaf area (leaf area/leaf mass) for sub-samples;
c. allometry (based on simple physical dimensions, such as stem diameter at breast height), using species-specific or stand-specific relationships based on detailed destructive measurement of a sub-sample of leaves, branches, or whole individuals;
d. indirect contact methods, such as plumb lines and inclined point quadrats; and
e. indirect non-contact methods, such as the Decagon Ceptometer (Decagon Devices, Inc., Pullman, Washington), the LI-COR LAI-2000 (Li-Cor, Inc., Lincoln, NE), and analysis of hemispheric photographs.

Methodologies A and B are commonly used in conjunction with definition 2 of LAI, whereas D and E are used with definitions 3 and 4, respectively. Methodology C may be used with any of the LAI definitions, including definition 1, depending upon the details of the calibration of the allometric equations.

The MODIS algorithm for LAI uses a three-dimensional radiative transfer model to describe canopy reflectance characteristics in multiple wavelength bands (Knyazikhin *et al.* 1998a, b). The model is inverted to determine LAI, using yet another approach not accounted for in the list above.

This study required repeated field measurements of the same location to observe seasonal and inter-annual change, obviously eliminating destructive measurement approaches. Allometry and litterfall methods would not be able to capture the timing of the seasonal change in leaf area. Because MODIS products have a 1 km

ground resolution, we also sought a field sampling technique that could rapidly characterize large areas. This led to the use of the LI-COR LAI-2000 that measures leaf area using an indirect non-contact method based on light transmittance through the canopy and assumptions of random leaf distribution within the canopy. This approach provided a repeatable consistent measure of effective LAI. This value of LAI was actually a total plant area index (PAI) as it lacked the ability to distinguish between green leaves and twigs or senescent leaves.

This study also examined temporal changes of f_{APAR}. The total absorbed photosynthetically active radiation (PAR) by a canopy (A_{PAR}) is the balance of the fluxes into and out of the canopy, expressed as:

$$A_{PAR} = Q_{in} + Q_b - Q_t - Q_r, \quad (1)$$

where Q_{in} is the incident PAR flux, Q_b is the PAR reflected into the canopy from the soil background, Q_t is the PAR transmitted through the canopy, and Q_r is the above-canopy reflected PAR (Hipps *et al.* 1983, Goward and Huemmrich 1992). PAR fluxes may be measured as energy fluxes ($W\,m^{-2}$) or as counts of photons with units of ($\mu mol\,m^{-2}\,s^{-1}$). To determine f_{APAR}, we normalize A_{PAR} by the incident PAR

$$f_{APAR} = A_{PAR}/Q_{in} = (Q_{in} + Q_b - Q_t - Q_r)/Q_{in}. \quad (2)$$

Frequently, Q_b is small and is set to zero in the calculation of f_{APAR} (e.g. Walter-Shea *et al.* 1992). In tall vegetation, it is often difficult to measure above canopy reflected PAR (Q_r). In that case, usually the fraction of intercepted PAR (f_{IPAR}) is calculated:

$$f_{IPAR} = (Q_{in} - Q_t)/Q_{in}. \quad (3)$$

Because PAR reflectance from vegetation (energy loss from the system) is usually small and somewhat cancelled out by the background reflectance (Q_b, energy gained by the system), f_{IPAR} is generally within a few percent of f_{APAR} (Huemmrich and Goward 1997, Huemmrich 2001). The patchy nature of light transmittance through woodland vegetation canopies means that large and spatially diverse samples of transmitted PAR (Q_t) and background reflected PAR (Q_b) must be collected to effectively describe these variables over a region.

As with the light-transmittance methods for determining LAI, the measurements of f_{APAR} cannot distinguish between PAR absorption by green leaves or non-green components of the canopy. This is a critical weakness of the field methods of f_{APAR} measurements because when modelling photosynthesis, the required information is the PAR absorbed by green leaves.

2. Site description

Surface observations were collected from the area surrounding the flux tower at the Kataba Local Forest, approximately 20 km south of Mongu in western Zambia. The tower was located at 15° 26.3′ S, 23° 15.2′ E, on a flat area adjacent to the Zambezi River flood plain. The land cover was miombo woodland on Kalahari Sand (Privette *et al.* 2002) or Kalahari woodland. Around the tower, the woodland tree and shrub basal area measured at chest height averaged $8.19\,m^2\,ha^{-1}$ with a standard deviation of $2.75\,m^2\,ha^{-1}$, for 42 samples, with canopy cover averaging 49.3% with a standard deviation of 10.6% (Scholes *et al.* 2002). There were five dominant species in the forest canopy: *Brachystegia spiciformis*, *Burkea africana*,

Guibourtia coleosperma, *Brachystegia bakerana*, and *Ochna pulchra*. The average upper canopy height was about 12 m. Beneath the canopy, there was a sparse understory of the grass *Pogonarthria squarrosa*, various shrubs and geoxylic suffrutices (*Copaifera baumiana*, *Paropsia brazzeana*, *Baphia massaiensis*, *Bauhinia petersiana* and *Lannea gossweileri*, among others), moss, and leaf litter. The soil was a pale grey, deep, excessively well-drained, fine sandy regosol of largely aeolian origin ('Kalahari sand') that showed almost no profile development with depth (Otter *et al*. 2002, Swap *et al*. 2002).

The site experiences a hot continental climate with pronounced wet and dry seasons. The average annual rainfall is 879 mm (Swap *et al*. 2002). Nearly all of the rain occurs from November to April, while typically no rainfall occurs from June to September. The forest vegetation is deciduous, responding to the seasonal variation in rainfall.

Ground measurements of LAI and f_{IPAR} were made along three parallel east–west running transects, each 750 m long. The transects were separated by 250 m. Each transect was divided up into thirty 25-m-long segments. The segments were used in the processing of the f_{IPAR} data, and the end-points of the segments were where the LAI-2000 measurements were collected (Privette *et al*. 2002). The length and spacing of the transects were chosen to sample an area large enough to be representative of a 1 km MODIS pixel.

3. Materials and methods

3.1 *Ground measurements*

Effective leaf area index was measured using the LI-COR LAI-2000 Plant Canopy Analyzer (PCA) (LI-COR Inc., Lincoln, Nebraska) instrument (Welles and Norman 1991). The LAI-2000 measures the intensity of blue light in five upward-looking concentric conical rings. Measurements made under the canopy were compared with open-sky measurements to determine transmittance for each of the five viewing angles. Effective leaf area was calculated from the transmittance in the different view angles based on the assumption of a random distribution of leaves. Measurements were collected near sunrise or sunset to obtain nearly uniform sky illumination. Open-sky measurements were collected before and after the transect measurements. This approach was chosen as it allows repeated consistent measurements of the same locations, without disturbing the canopy. This made possible LAI measurements to be collected throughout the growing season to examine LAI phenology.

Ground-level measurements were made at fixed locations every 25 m along the transects. Effective LAI values were determined for each measurement, and all 93 values were averaged to estimate the MODIS pixel LAI (Privette *et al*. 2002). LAI-2000 measurements were rejected when they were collected under partly cloudy conditions, when open-sky measurements were not available at both the beginning and ending of the transect measurements, or when the sky became too dark for meaningful transmittance values to be determined.

The Tracing Architecture and Radiation of Canopies (TRAC) (3rd Wave Engineering, Nepean, Canada) instrument was used to measure f_{APAR} and f_{IPAR}. Generally, TRAC data would be processed using proprietary software to determine gap fraction distribution, and from that LAI and leaf clumping factors (Chen and Cihlar 1995, Chen 1996, Chen *et al*. 2000). Previous studies had already described LAI for this site using the TRAC (Privette *et al*. 2002), while f_{APAR} had not been examined.

In this study, the raw TRAC data were processed in a different way to calculate f_{IPAR}. The TRAC head contained three pyranometers sensitive to PAR wavelengths, with two sensors upward looking and one downward looking (Chen *et al.* 2000). It was carried through the forest along a transect at a steady walking pace while the sensors measured PAR at 32 Hz, resulting in a horizontal sampling interval of about 1.7 cm (Privette *et al.* 2002). The sensors were held about 0.7 m off the ground. After each 25 m segment along the transect, the operator entered a date/time stamp into the data by pressing a button. TRAC measurements were collected on clear days. If a cloud obscured the Sun, data collection was paused until the cloud passed.

f_{IPAR} from TRAC was calculated using equation (3). PAR transmittance values were determined from the upward viewing pyranometers on the TRAC instrument. Owing to the large gaps in the canopy, incident PAR was estimated from the TRAC data as 95% of the maximum upward-viewing pyranometer value for each transect. The 95% factor was used to adjust for the TRAC not being completely level in each measurement. As TRAC data were collected over a relatively short period of time, with each transect measurement set taking less than a half hour to collect, the incident PAR (Q_{in}) was considered constant over the period of time covered to measure each 750 m transect. With a value for incident PAR determined for a transect measurement set, each upward-viewing pyranometer measurement was used as a value of Q_{t}. f_{IPAR} values greater than one were set to one. Approximately 40 000 samples were collected in a single transect measurement set, and the f_{IPAR} values for each of these observations were averaged to give a transect-average f_{IPAR} value. The three transect average f_{IPAR} values were averaged together to provide a site f_{IPAR} value.

To calculate f_{APAR}, measurements of above-canopy PAR albedo were required as well as the PAR reflected from the background. PAR albedo was estimated with data from upward and downward viewing pyranometers (Model CM14, Kipp & Zonen, Delft, The Netherlands) that measured the entire shortwave flux and the near-infrared part ($>0.7\,\mu$m) of the shortwave. The pyranometers were located on $\sim$2 m arms extending outward from the top of a 30 m tower positioned midway between the centres of the middle and southern transects. The pyranometers effectively integrate radiances over the hemisphere, which in the current configuration provides a $\sim$200 m diameter circular footprint for 0–80° incident angles. There was no measurement of the spatial variation of the PAR albedo, so the single value from the flux tower was used to describe all transects. PAR flux values were taken to be the differences between the shortwave and near-infrared fluxes, so that PAR albedo ($Q_{\mathrm{r}}/Q_{\mathrm{in}}$) was calculated as:

$$Q_{\mathrm{r}}/Q_{\mathrm{in}} = (Q_{\mathrm{swr}} - Q_{\mathrm{nirr}})/(Q_{\mathrm{swin}} - Q_{\mathrm{nirin}}), \tag{4}$$

where Q_{swr} was the reflected short wave flux above the canopy, Q_{swin} was the incident short wave flux, Q_{nirr} was the reflected near-infrared flux above the canopy, and Q_{nirin} was the incident near-infrared flux. Shortwave pyranometers measure a wavelength range of 0.285–2.8 μm, while the lower wavelength boundary for PAR is defined as 0.4 μm. This means that the tower estimates of PAR flux include some ultraviolet wavelengths. As the atmosphere blocks most of the incident ultraviolet radiation from reaching the ground, we assume that this addition to the PAR flux estimation is small.

Besides measuring transmitted PAR, the TRAC instrument measured reflected background PAR, the other component of f_{APAR}. The challenge to calculating

f_{APAR} was to combine the TRAC and tower data. The tower sensors were not intercalibrated to the PAR sensors in the TRAC; in fact the tower sensors measured energy units ($W\,m^{-2}$) while the TRAC measured number of quanta (photons) ($\mu mol\,s^{-1}\,m^{-2}$). To account for these two data sources, the f_{APAR} equation (equation (2)) was rearranged to work with self-consistent, unitless ratios and avoid mixing data from the different sources:

$$f_{APAR} = Q_{in}/Q_{in} + Q_b/Q_{in} - Q_t/Q_{in} - Q_r/Q_{in} \quad (5)$$

or

$$f_{APAR} = f_{IPAR} + Q_b/Q_{in1} - Q_r/Q_{in2}. \quad (6)$$

The background reflectance (Q_b/Q_{in1}) came from TRAC data and was calculated using a similar approach to the f_{IPAR}. As with f_{IPAR}, the average measured PAR reflected from the ground and the maximum transmitted PAR were determined. Incident PAR (Q_{in1}) was assumed to be 95% of maximum transmitted PAR for the transect. In equation (6), the incident PAR (Q_{in2}) in the PAR albedo term (Q_r/Q_{in2}) came from the tower measurements. PAR albedo values from the tower fluxes were recorded as 15 min averages. These were matched to the TRAC measurement times to within less than an hour. So, two different values were used for the incident PAR (Q_{in}), but they were used to normalize the data from two different instruments.

3.2 *Satellite measurements*

The MODIS LAI and f_{APAR} products (Terra satellite, MOD15, level 4, collection 3) were produced at 1 km spatial resolution over 8 day compositing periods (Myneni *et al.* 2002). The algorithm used to produce these products was based on the inversion of a three-dimensional radiative transfer model. The LAI and f_{APAR} products retrieved from the algorithm represent values for green leaves under direct solar illumination, with LAI being half the total leaf surface area per unit ground area. Algorithm inputs included atmospherically corrected bidirectional reflectance values in two wavelength bands, red and near-infrared; the Sun and viewing geometry for the reflectance data; and a land cover classification that defined the basic vegetation architecture and characteristics. For a range of canopy structures and background reflectances that were expected from natural conditions, the algorithm determined canopy reflectances and compared them with observations. In cases where the differences between modelled and observed reflectances were within the uncertainty of the observed reflectance, the biophysical values used as inputs were considered as possible solutions. A test of energy conservation was also applied. The mean LAI and f_{APAR} of possible solutions were reported as the MODIS products (Knyazikhin *et al.* 1998a, b).

The MODIS NDVI product (Terra satellite, MOD13, level 3, collection 3) was also examined in this study, as NDVI has long been used in studies to determine LAI or f_{APAR} (for example, Hatfield *et al.* 1984, Badhwar *et al.* 1986, Peterson *et al.* 1987, Wiegand *et al.* 1990, Goward and Huemmrich 1992). This product provided a check on the use of MODIS NDVI as an inter-seasonal correlate to these variables in African woodlands. The MODIS NDVI product has a spatial resolution of 1 km with a 16 day compositing period. The inputs are red and near-infrared surface reflectances, corrected for molecular scattering, ozone absorption, and aerosols, and adjusted to nadir with the use of bi-directional reflectance function models (Huete *et al.* 2002).

Both the LAI and f_{APAR} product and NDVI are sensitive to the green leaves in the canopy. Green leaves have large differences in radiation absorption between the red and near-infrared bands, while in dead leaves and soil, that difference is decreased. Algorithms use this difference to determine LAI and f_{APAR}. As described above, the ground measurements do not distinguish between green and non-green canopy materials. This is a critical difference between the ground measurements and the satellite values.

In this study, individual values of the 1 km pixel for both the NDVI and LAI/f_{APAR} products representing the Mongu tower site were extracted and used for the comparison with the ground measurements. MODIS geolocation of pixels is approximately 50 m at nadir, a very small value compared with the pixel size (Wolfe *et al.* 2002). In the LAI/f_{APAR} algorithm, the land cover classification of the Mongu tower site was identified as savannah, as were the pixels surrounding the site. Each pixel used had a quality assessment code associated with it. MODIS products were not used if the quality assessments indicated significant cloud contamination or poor data quality, or if the primary algorithm was not used.

4. Results

4.1 f_{IPAR}

Measurements with the TRAC began in February of 2000 and were generally collected at monthly intervals thereafter. Comparison of the time series of average f_{IPAR} values from ground measurements and the MODIS f_{APAR} from the start of the data collection into 2002 (figure 1) showed that the ground and MODIS data followed similar seasonal patterns through time. However, there was a significant offset between the ground-measured f_{IPAR} and satellite-measured f_{APAR} values. TRAC values of f_{APAR} ranged from a minimum of 0.21 to a maximum of 0.64, while the MODIS values were between 0.41 and 0.96, with the satellite values consistently higher (~0.2 absolute) than the ground observations.

The standard deviation of all of the segment values making up the average provided an indication of the f_{IPAR} variability within the pixel. The TRAC f_{IPAR} standard deviations were between 0.15 and 0.25. The standard deviations of the nine

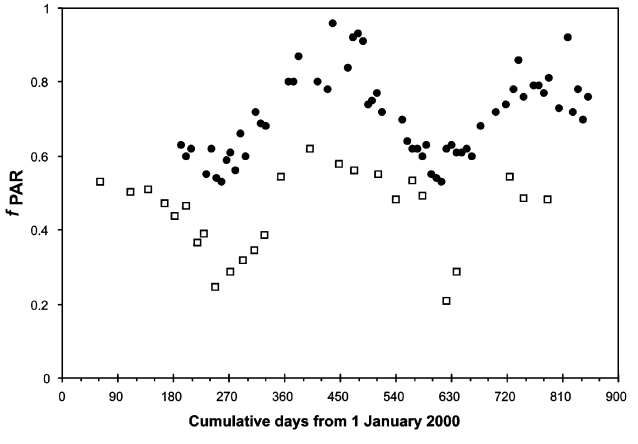

Figure 1. f_{PAR} values for the Mongu site over time. f_{PAR} data from ground measurements (□) and derived from MODIS observations (●).

surrounding MODIS pixels gave a measure of the regional variability, and these values were between 0.01 and 0.17. As expected for this type of open woodland, the standard deviations indicate more spatial variation at the 25 m segment scale than at the scale of the larger 1 km MODIS pixels.

In figure 2, there was a direct comparison between the ground measured f_{IPAR} values with MODIS values where the TRAC measurements were collected during the MODIS product 8 day compositing period. The points were well away from the 1-to-1 line. The MODIS f_{APAR} values were higher with a smaller range than the ground measurements. The MODIS and ground measurements of f_{IPAR} tended to be closest at high values of f_{IPAR}.

4.2 *LAI*

Ground measurements with LAI-2000 began in October of 2000. The MODIS LAI product became available starting in June of 2000. Figure 3 shows the LAI over time from the ground measurements using the LAI-2000 and the MODIS LAI for the single 1 km pixel of the Mongu tower site. The short-term variability from consecutive MODIS LAI observations was due to uncertainties in input data and the algorithm.

Over the course of a year, the LAI pattern from both sources showed a strong seasonal variation. The highest values of LAI occurred in the peak wet season (January through March) with the canopy LAI reaching values around 2. Following this, there was a steady decline in LAI to approximately 1 in September.

There were eight times where the ground measurement occurred during the 8 day period where the MODIS result was assigned a good quality code, allowing a direct comparison between the two measures of LAI. These points were plotted in figure 4 and showed a strong relationship between the ground-measured effective LAI and the MODIS LAI, with the MODIS LAI giving a value slightly higher than the ground LAI. This offset may be because the ground LAI was an effective LAI and did not include a clumping factor (Chen and Cihlar 1995). However, the LAI-2000 measurements actually provide Plant Area Index (sum of leaf and stem area) rather

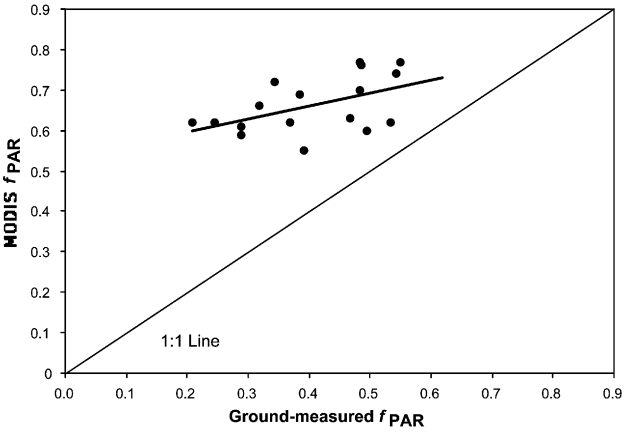

Figure 2. MODIS f_{PAR} and ground measured f_{PAR} values where the ground measurements were collected during the 8 day compositing period of the MODIS value. $y=0.32x+0.53$; $R^2=0.26$; $n=21$.

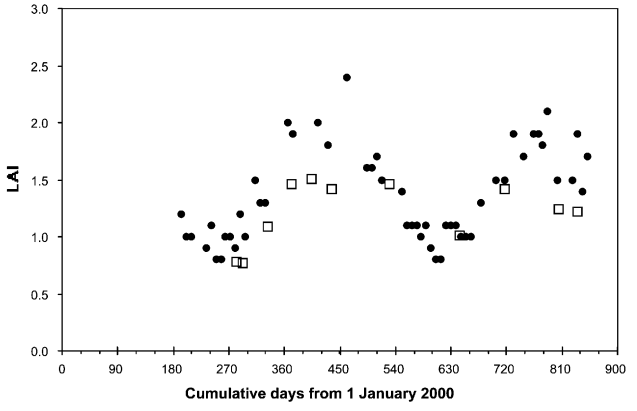

Figure 3. LAI values for the Mongu site over time. LAI data from ground measurements (□) and derived from MODIS observations (●).

than the green leaf area index estimated from MODIS. Therefore, the LAI-2000 results should be slightly greater (e.g. by about 0.3) than the MODIS LAI results.

4.3 *NDVI, f_{IPAR} and LAI*

Rather than using a model inversion approach, another method for determining LAI and f_{IPAR} by remote sensing has been to correlate the variables with NDVI. We compared the seasonal pattern of the MODIS 16-day composite NDVI with the ground-measured values of LAI and f_{IPAR} in figure 5. Direct comparisons between the MODIS NDVI and the ground-based measurements collected during the compositing period displayed good correlations of LAI and f_{IPAR} with NDVI (figures 6 and 7).

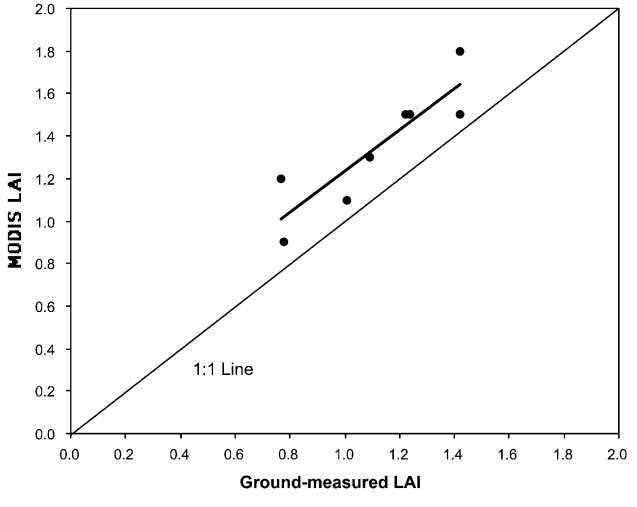

Figure 4. MODIS LAI and ground measured LAI values where the ground measurements were collected during the 8 day compositing period of the MODIS value.
$y=0.98x+0.25$; $R^2=0.79$; $n=8$.

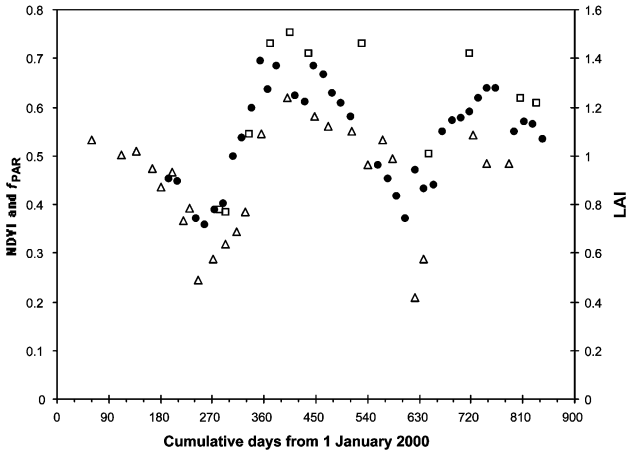

Figure 5. NDVI, f_{PAR}, and LAI values for the Mongu site over time. LAI (□) and f_{PAR} (Δ) data from ground measurements and MODIS NDVI (●).

5. Discussion

A comparison of the ground-based measurements of LAI and f_{IPAR} with the MODIS algorithm results showed that the MODIS algorithm provided a good estimate of LAI, but has a significant f_{IPAR} bias. As f_{IPAR} is directly related to the amount of leaf area in the canopy intercepting light, it was surprising that there should be this discrepancy. We examined several possible causes for differences between the MODIS f_{APAR} and ground-measured f_{IPAR}.

One possible cause of the offset between the MODIS algorithm, that determines f_{APAR}, and the surface-measured f_{IPAR} was the difference between the intercepted and absorbed PAR. To examine this difference, we calculated f_{APAR} for individual transects at times when flux data above the canopy from the tower were also

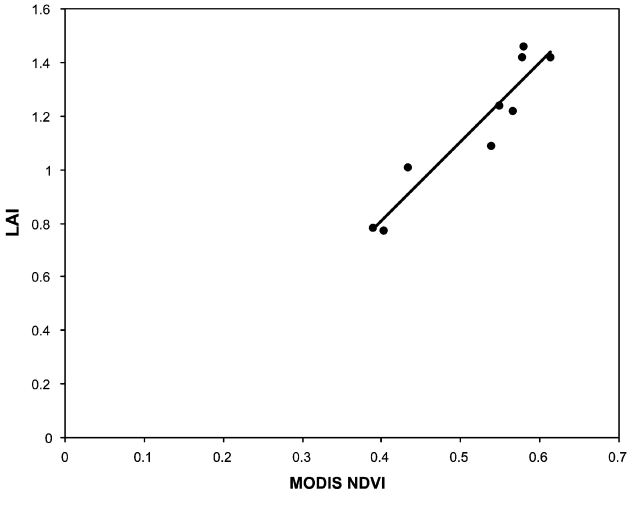

Figure 6. MODIS NDVI and ground measured LAI values where the ground measurements were collected during the 16 day compositing period of the MODIS value. $y=2.97x-0.38$; $R^2=0.90$; $n=9$.

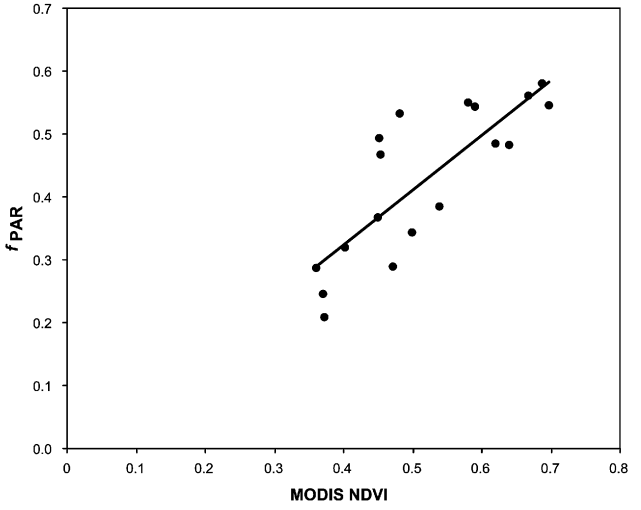

Figure 7. MODIS NDVI and ground measured f_{PAR} values where the ground measurements were collected during the 16 day compositing period of the MODIS value. $y=0.88x+0.03$; $R^2=0.66$; $n=18$.

available. There were 28 cases where we were able to calculate f_{APAR} for a transect. There was very little difference in values between f_{IPAR} and f_{APAR} (figure 8). The largest difference was around 4% f_{APAR}. The small difference between intercepted and absorbed PAR was because an increase in PAR coming into the canopy through reflectance from the ground (an average of about 6% reflectance) was just about offset by the above canopy reflected PAR (an average of about 5%).

Solar zenith angle (SZA) variations may have an effect on the measurement of f_{IPAR} (Goward and Huemmrich 1992). Ideally, f_{IPAR} measurements should all be

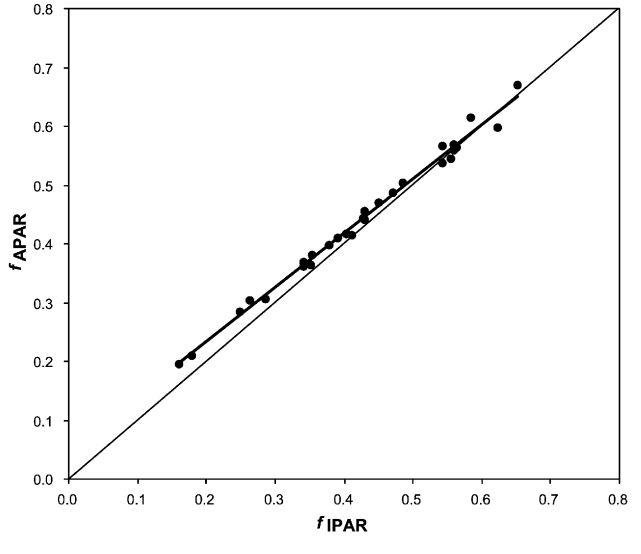

Figure 8. f_{IPAR} vs. f_{APAR}. Data from individual transects A, B, and C are used in this plot, i.e. each point represents the value for a single transect.
$y=0.99x+0.05$; $R^2=0.99$; $n=28$.

collected at the same SZA for seasonal comparisons, or matching the SZA of the satellite overpass time for comparisons between ground and satellite, but in practice it is difficult to keep to such an exacting schedule. Since the data were collected under a variety of SZA, it is important to evaluate the magnitude of their effect. The best way to examine the relationship between SZA and f_{IPAR} would be to measure f_{IPAR} several times in the same day, so that SZA varies while the overall canopy characteristics have not changed. However, such measurements were not collected. With the available data, we assumed for a null hypothesis that SZA does significantly affect f_{IPAR}. Measurements from individual 750 m transects were examined, as these measurements were collected over time periods of ~30 min compared with the time over which all three transects were measured, which could be hours. This allowed a specific value of SZA to be assigned to a transect measurement. To test the hypothesis, periods over which there were small changes in f_{IPAR} were chosen. Five periods were identified where there were small changes in f_{IPAR}: for transect A, cumulative days 271–326 and cumulative days 454–540; transect B, days 60–181; and transect C, cumulative days 138–199 and 354–472. All of these periods were when leaves were out in the forests. The measured f_{IPAR} for those periods were plotted against SZA (figure 9) and showed significant variations in SZA with a very small variation in f_{IPAR}. The null hypothesis was therefore rejected, as there was no indication that differences in SZA would result in significant differences in f_{IPAR} for any of the transects.

Another possible difference between the MODIS product and ground-measured f_{IPAR} was that the model for the MODIS product used energy units in the calculations, while the TRAC PAR detectors are quantum sensors that count photons. The energy in a photon is related to its wavelength, and photons with shorter wavelengths have more energy than photons with longer wavelengths. This means that the TRAC sensors register a count for a photon of blue light the same as a photon of red light, even though the blue light photon has over 40% more energy than the red light photon. No data were collected on the spectral distribution of the incident or absorbed light, so a direct analysis was not possible. We examined this problem using the GeoSail model (Huemmrich 2001) to describe canopy spectral absorption for a variety of canopy geometries, both continuous and clumped. The model was formulated to calculate the fraction of the incident radiation absorbed by

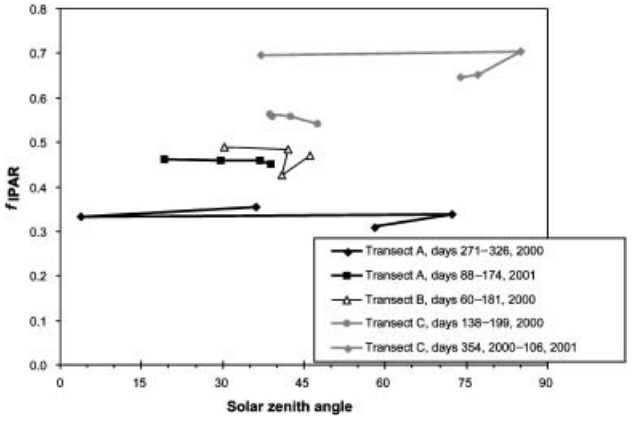

Figure 9. Transect f_{IPAR} vs. solar zenith angle for five periods where individual transect f_{IPAR} had small changes over time.

the canopy for wavelength bands of 0.005 μm between 0.400 and 0.700 μm (61 bands). Test cases used a variety of measured values for leaf optical properties over a range of LAI values. A typical model result is shown in figure 10.

The results of the canopy model runs suggested that the spectral absorptance of canopies of green leaves over the PAR wavelengths was fairly flat over the PAR wavelengths. No spectral region was more than a few percent different from the average. Generally, the largest difference in spectral absorption was in the green wavelengths. However, there was no indication that measuring f_{APAR} by photon counts versus measuring by energy units produced differences greater than 1% (see figure 10).

The TRAC-derived f_{IPAR} does not account for vegetation between the ground surface and ~0.7 m, the height of the sensors during sampling. This error does not occur with the LAI-2000, since that sensor was placed at ground level during operation. The MODIS products represent the full vertical column of vegetation. Nevertheless, understory vegetation is considerably more sparse than overstory vegetation at Mongu, and therefore its contribution to the total column f_{IPAR} is likely to be small.

The relationships between LAI and f_{IPAR} for both the ground-based and MODIS values were examined in figure 11. As both the MODIS LAI and f_{APAR} come from the same algorithm, it was not surprising that there is a tight relationship between them. The relationship between the ground-measured values was more scattered, but still strong considering that the ground-based LAI and f_{IPAR} were measured with different instruments, at different times, and often on different days. Figure 11 clearly showed that there was a different relationship between LAI and f_{IPAR} for the ground-based measurements in comparison with the MODIS algorithm.

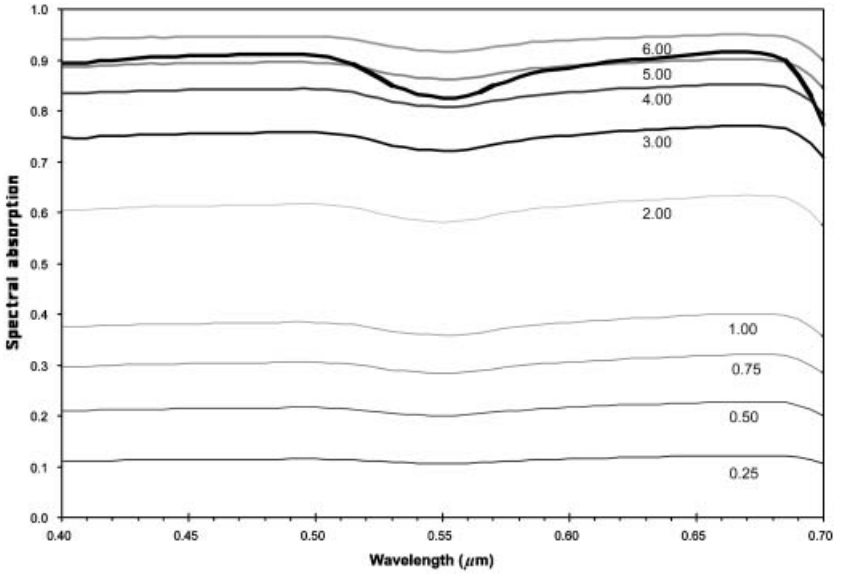

Figure 10. Model results of spectral absorption by vegetation canopies over PAR wavelengths. The modelled canopy consisted of a single, horizontally infinite layer of leaves. The leaves had a spherical leaf inclination angle distribution. Each line represents a canopy with the LAI shown below the line. The dark black line was the individual leaf absorptance used as model input.

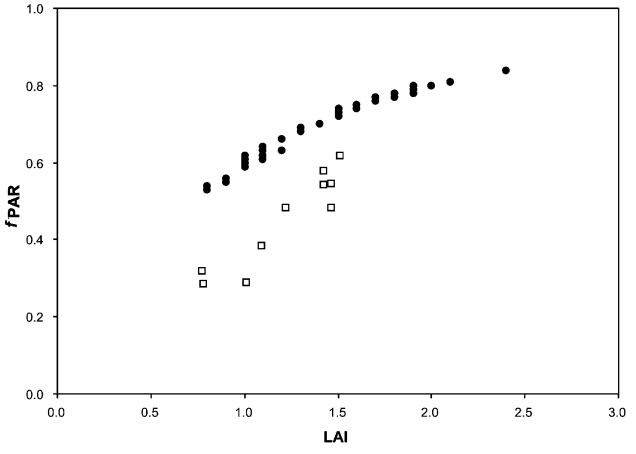

Figure 11. LAI and f_{APAR} or f_{IPAR} values for the same time periods. □: ground-measured values; ●: from the MODIS algorithm.

A simple canopy reflectance model was used to illustrate possible causes of the differences between the measured LAI/f_{APAR} relationship and that derived from the MODIS algorithm. Again, the GeoSail model (Huemmrich 2001) was used. The simulation results shown in figure 12 assumed a landscape that was a plane covered with identical trees described as cylinders with a height to width ratio of 4; all the leaf area was constrained within the cylinders; the leaves had a spherical leaf angle distribution; and SZA was 30°. In each of the simulations, represented by a line in figure 12, the canopy coverage (that is the area of the plane covered by cylinders) was held constant with LAI varying by increasing the LAI per tree (leaf density).

The results from this simple model showed that different LAI/f_{APAR} curves were formed depending on the canopy coverage. These simulations suggest that the differences between the MODIS LAI and f_{APAR} and ground-measured values may be due to an error in the estimate of canopy cover in the MODIS algorithm.

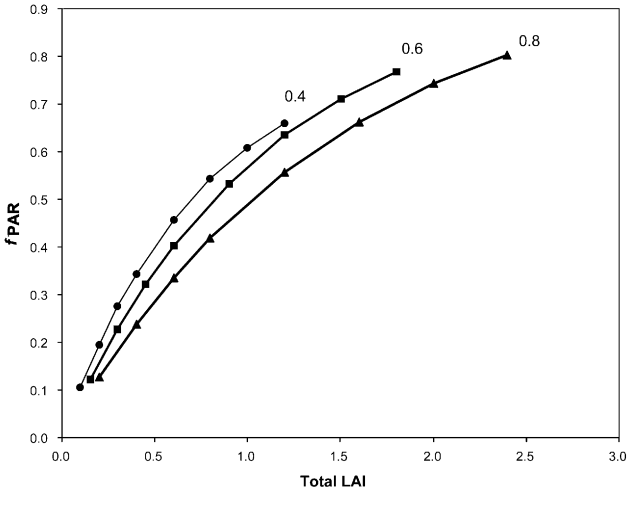

Figure 12. GeoSail simulations of LAI and f_{APAR} for deciduous forest canopies. The fraction of canopy coverage for each line is shown above the line.

Figure 12 showed that the same LAI value can have different values of f_{APAR} depending on the fractional canopy cover. If the MODIS algorithm underestimated fractional canopy cover, it may well overestimate f_{APAR} for a given LAI (compare figures 11 and 12). The measured fractional canopy cover when the canopy was fully leafed out was 0.49 (Scholes *et al.* 2002), while the range of fraction of canopy cover in the MODIS algorithm for the savannah biome was 0.2–0.4 (Knyazikhin *et al.* 1998b). Thus, for the purposes of the MODIS algorithm, the classification of the Mongu site as savannah was an error that leads to the observed problems with the f_{APAR} values.

Beyond the effect of canopy structure, another source of uncertainty was indicated in the relationship between NDVI and f_{IPAR}. Some of the scatter in the NDVI/f_{IPAR} relationship shown in figure 7 may be explained by dividing the data between the green-up periods and dry periods. The green-up periods were the times when NDVI was increasing, and the dry periods were when NDVI was flat or decreasing. Figure 13 shows the same data as figure 7 but with two lines describing NDVI/f_{IPAR} relationships, one during the green-up and the other during dry periods.

During the green-up, the woodland in Mongu went from nearly leafless to fully green. This period was characterized by a tight relationship between NDVI and f_{IPAR}. During the dry periods, the leaves drooped, dried out, and became brown, while there were leaves, even dead ones, on the trees they were intercepting PAR and contributing to the f_{IPAR}. However, NDVI is sensitive to the amount of green foliage, so NDVI dropped during the dry period more than the decrease in f_{IPAR}. This produced the second relationship in figure 13 shown as the dry line. Over the year in Mongu, starting at the time of no leaves, the trees greened up, increased green LAI and f_{IPAR} and caused a steady increase in NDVI. As the dry season began, NDVI decreased faster than f_{IPAR}, resulting in a relationship line with a lower slope. Finally, the trees lost their dead leaves, and f_{IPAR} suddenly dropped with little change in NDVI, bringing the cycle back to the start. This cycle suggests

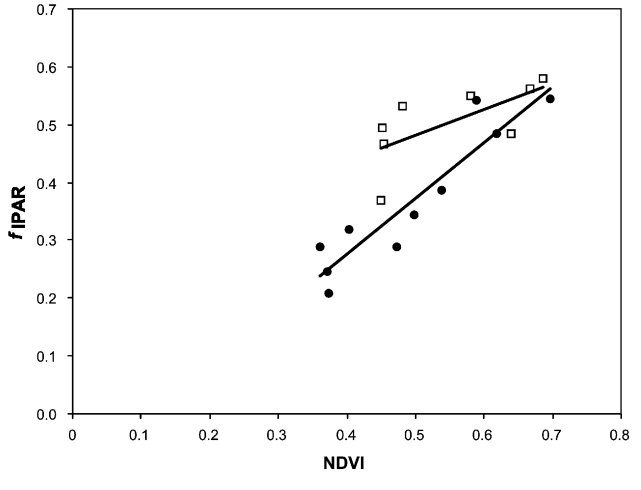

Figure 13. MODIS NDVI and ground measured f_{IPAR} values where the ground measurements were collected during the 16 day compositing period of the MODIS value. ●: points that occur during the green-up period. $y=0.96x-0.11$; $R^2=0.87$; $n=10$; □: data points collected during the dry periods. $y=0.44x-0.26$; $R^2=0.45$; $n=8$.

that seasonal variations in leaf optical properties due to drying are not fully accounted for in the MODIS algorithm.

6. Conclusions

This study of seasonal variation in MODIS LAI and f_{APAR} products shows that both products describe the pattern of seasonal vegetation change observed at Mongu. However, we find that while the MODIS LAI product matches observed values of ground-measured effective LAI with a small offset, there are significant differences between the MODIS f_{APAR} product and ground-measured f_{IPAR}.

The examination of the relationship between NDVI and f_{IPAR} indicated that variations in leaf optical properties may be an important source of error in retrieving biophysical variables (Goward and Huemmrich 1992, Huemmrich and Goward 1997). The spatial and temporal variability of leaf optical properties is not well known. Improving the accuracy of biophysical variable retrieval may require a systematic study of the variability of leaf optical properties.

This study examined the effects of SZA on f_{IPAR} indirectly; future validation studies should directly address this issue. Data-collection protocols should include f_{IPAR} measurements at multiple times in a single day at a single site to test the effects of SZA on f_{IPAR}.

Simulations from a simple canopy reflectance model suggest that another possible cause of the differences between MODIS and ground-measured f_{IPAR} may be due to errors in estimating canopy cover in the MODIS algorithm. The canopy cover differences are due to the classification of Mongu as a savannah where the assigned fractional canopy cover in the algorithm was less than the observed coverage.

The results of this analysis clearly show that success in retrieving one biophysical variable does not ensure success with other variables, even when there is a physical link between the variables as there is between LAI and f_{APAR}. This means that validation efforts must be made for all satellite data products.

Acknowledgements

This study was part of the SAFARI 2000 Initiative and was funded under the EOS Validation Program. All field data used in this study are on the SAFARI 2000 CD-ROM Volume III, available from the Oak Ridge National Laboratories Data Active Archive Center (DAAC): ORNL DAAC User Services Office, Oak Ridge National Laboratory, PO Box 2008, Mail Stop 6407, Oak Ridge, TN 37831-6490, USA. Email: ornl@eos.nasa.gov

References

BADHWAR, G.D., MACDONALD, R.B., HALL, F.G. and CARNES, J.G., 1986, Spectral characterization of biophysical characteristics in a boreal forest: Relationship between Thematic Mapper band reflectance and leaf area index for aspen. *IEEE Transactions on. Geoscience and Remote Sensing*, **24**, pp. 322–326.

BARCLAY, H.J., 1998, Conversion of total leaf area to projected leaf area in lodgepole pine and Douglas-fir. *Tree Physiology*, **18**, pp. 185–193.

CHEN, J.M., 1996, Optically-based methods for measuring seasonal variation in leaf area index in boreal conifer stands. *Agricultural and Forest Meteorology*, **80**, pp. 135–163.

CHEN, J.M. and CIHLAR, J., 1995, Plant canopy gap size analysis theory for improving optical measurements of leaf area index. *Applied Optics*, **34**, pp. 6211–6222.

CHEN, J.M., LEBLANC, S.G. and KWONG, M., 2000, *Manual for TRAC* (Ottawa: Canada Centre for Remote Sensing).

CHIDUMAYO, E.N., 2001, Climate and phenology of savanna vegetation in southern Africa. *Journal of Vegetation Science*, **12**, pp. 347–354.

CHURKINA, G. and RUNNING, S.W., 1998, Contrasting climatic controls on the estimated productivity of global terrestrial biomes. *Ecosystems*, **1**, pp. 206–215.

GOWARD, S.N. and HUEMMRICH, K.F., 1992, Vegetation canopy PAR absorptance and the normalized difference vegetation index: an assessment using the SAIL model. *Remote Sensing of Environment*, **39**, pp. 119–140.

GOWARD, S.N., TUCKER, C.J. and DYE, D.G., 1985, North American vegetation patterns observed with the NOAA-7 advanced very high resolution radiometer. *Vegetatio*, **64**, pp. 3–14.

HATFIELD, J.L., ASRAR, G. and KANEMASU, E.T., 1984, Intercepted photosynthetically active radiation estimated by spectral reflectance. *Remote Sensing of Environment*, **14**, pp. 65–75.

HIPPS, L.E., ASRAR, G. and KANEMASU, E., 1983, Assessing the interception of photosynthetically active radiation in winter wheat. *Agricultural Meteorology*, **28**, pp. 253–259.

HUEMMRICH, K.F., 2001, The GeoSail model: a simple addition to the SAIL model to describe discontinuous canopy reflectance. *Remote Sensing of Environment*, **75**, pp. 423–431.

HUEMMRICH, K.F. and GOWARD, S.N., 1997, Vegetation canopy PAR absorptance and NDVI: an assessment for ten tree species with the SAIL model. *Remote Sensing of Environment*, **61**, pp. 254–269.

HUETE, A., DIDAN, K., MIURA, T., RODRIGUEZ, E.P., GAO, X. and FERREIRA, L.G., 2002, Overview of the radiometric and biophysical performance of the MODIS vegetation indices. *Remote Sensing of Environment*, **83**, pp. 195–213.

JUSTICE, C.O., TOWNSHEND, J.R.G., HOLBEN, B.N. and TUCKER, C.J., 1985, Analysis of the phenology of global vegetation using meteorological satellite data. *International Journal of Remote Sensing*, **6**, pp. 1271–1381.

KNYAZIKHIN, Y., MARTONCHIK, J.V., DINER, D.J., MYNENI, R.B., VERSTRAETE, M., PINTY, B. and GOBRON, N., 1998a, Estimation of leaf area index and fraction absorbed photosynthetically active radiation from atmosphere corrected MISR data. *Journal of Geophysical Research*, **103**, pp. 32239–32256.

KNYAZIKHIN, Y., MARTONCHIK, J.V., MYNENI, R.B., DINER, D.J. and RUNNING, S.W., 1998b, Synergistic algorithm for estimating vegetation canopy leaf area index and fraction absorbed photosynthetically active radiation from MODIS and MISR data. *Journal of Geophysical Research*, **103**, pp. 32257–32274.

MOULIN, S., KERGOAT, L., VIOVY, N. and DEDIEU, G., 1997, Global-scale assessment of vegetation phenology using NOAA/AVHRR satellite measurements. *Journal of Climate*, **10**, pp. 1154–1170.

MYNENI, R.B., KNYAZIKHIN, Y., PRIVETTE, J., GLASSY, J., TIAN, Y., WANG, Y., HOFFMAN, S., SONG, X., ZHANG, Y., SMITH, G.R., LOTSKCH, A., FRIEDL, M., MORISETTE, J.T., VOTAVA, P., NEMANI, R.R. and RUNNING, S.W., 2002, Global products of vegetation leaf area and fraction absorbed PAR from year one of MODIS data. *Remote Sensing of Environment*, **83**, pp. 214–231.

OTTER, L.B., SCHOLES, R.J., DOWTY, P., PRIVETTE, J., CAYLOR, K., RINGROSE, S., MUKELABAI, M., FROST, P., HANAN, N., TOTOLO, O. and VEENENDAAL, E.M., 2002, The Southern African Regional Science Initiative (SAFARI 2000): wet season campaigns. *South African Journal of Science*, **98**, pp. 131–137.

PETERSON, D.L., SPANNER, M.A., RUNNING, S.W. and TEUBER, K.B., 1987, Relationship of Thematic Mapper Simulator data to leaf area index of temperate coniferous forest. *Remote Sensing of Environment*, **22**, pp. 323–341.

POTTER, C.S., RANDERSON, J.T., FIELD, C.B., MATSON, P.A., VITOUSEK, P.M., MOONEY, H.A. and KLOOSTER, S.A., 1993, Terrestrial ecosystem production—a process model-based on global satellite and surface data. *Global Biogeochemical Cycles*, **7**, pp. 811–841.

PRIVETTE, J.L., MYNENI, R.B., KNYAZIKHIN, Y., MUKUFUTE, M., ROBERTS, G., TIAN, Y., WANG, Y. and LEBLANC, S.G., 2002, Early spatial and temporal validation of MODIS LAI product in Africa. *Remote Sensing of Environment*, **83**, pp. 232–243.

REED, B.C., BROWN, J.F., VANDERZEE, D., LOVELAND, T.R., MERCHANT, J.W. and OHLEN, D.O., 1994, Measuring phenological variability from satellite imagery. *Journal of Vegetation Science*, **5**, pp. 703–714.

SCHOLES, R.J., DOWTY, P.R., CAYLOR, K., PARSONS, D.A.B., FROST, P.G.H. and SHUGART, H.H., 2002, Trends in savanna structure and composition along an aridity gradient in the Kalahari. *Journal of Vegetation Science*, **13**, pp. 419–428.

SCURLOCK, J.M.O., ASNER, G.P. and GOWER, S.T., 2001, *Worldwide Historical Estimates of Leaf Area Index, 1932–2000, Oak Ridge National Laboratory Technical Report ORNL/TM-2001/268*.

SWAP, R.J., ANNEGARN, H.J., SUTTLES, J.T., HAYWOOD, J., HELMLINGER, M.C., HELY, C., HOBBS, P.V., HOLBEN, B.N., JI, J., KING, M.D., LANDMANN, T., MAENHAUT, W., OTTER, L., PAK, B., PIKETH, S.J., PLATNICK, S., PRIVETTE, J., ROY, D., THOMPSON, A.M., WARD, D. and YOKELSON, R., 2002, The Southern African Regional Science Initiative (SAFARI 2000): overview of the dry season field campaign. *South African Journal of Science*, **98**, pp. 125–130.

WALTER-SHEA, E.A., BLAD, B.L., HAYS, C.J., MESARCH, M.A., DEERING, D.W. and MIDDLETON, E.M., 1992, Biophysical properties affecting vegetative canopy reflectance and absorbed photosynthetically active radiation at the FIFE site. *Journal of Geophysical Research-Atmospheres*, **97**, pp. 18925–18934.

WELLES, J.M. and NORMAN, J.M., 1991, Instrument for indirect measurement of canopy architecture. *Agronomy Journal*, **83**, pp. 818–825.

WIEGAND, C.L., GERBERMANN, A.H., GALLO, K.P., BLAD, B.L. and DUSEK, D., 1990, Multisite analyses of spectral-biophysical data for corn. *Remote Sensing of Environment*, **33**, pp. 1–16.

WOLFE, R.E., NISHIHAMA, M., FLEIG, A.J., KUYPER, J.A., ROY, D.P., STOREY, J.C. and PATT, F.S., 2002, Achieving sub-pixel geolocation accuracy in support of MODIS land science. *Remote Sensing of Environment*, **83**, pp. 31–49.